

Shipboard LADCP/ χ pod Profiling of Internal Wave Structure and Dissipation in the Luzon Strait

Jonathan D. Nash & James N. Moum
College of Oceanic & Atmospheric Sciences
Oregon State University
Corvallis OR 97331-5503
ph: (541) 737-4573 fx: (541) 737-2064
email: nash@coas.oregonstate.edu

Awards: N00014-09-1-0281
and N00014-11-1-0367 (Early Student Support)
<http://mixing.coas.oregonstate.edu/>

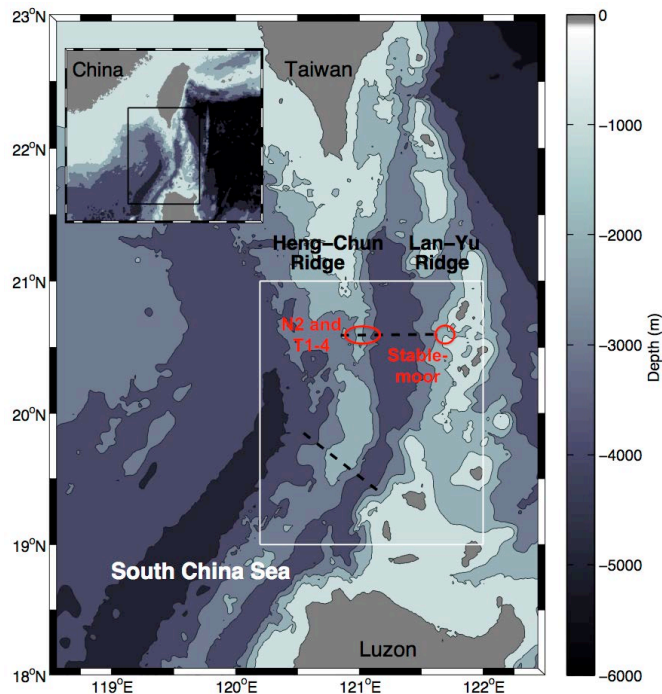
LONG-TERM GOALS

We seek a more complete and fundamental understanding of the hierarchy of processes that transfer energy and momentum from large scales, feed the internal wavefield, and ultimately dissipate through turbulence. This cascade impacts the acoustic, optical, and biogeochemical properties of the water column, and feeds back to alter the larger scale circulation. Studies within the **Ocean Mixing Group** at OSU emphasize observations, innovative sensor / instrumentation development and integration, and process-oriented internal wave and turbulence modeling for interpretation.

OBJECTIVES

Luzon Strait represents a major source of internal tides and NLIWs in the SCS. However, unlike other regions of strong internal wave generation (i.e., Hawaii), Luzon Strait is believed to be highly dissipative. We seek to understand the character of this enhanced nonlinearity and turbulence, and how it affects internal wave generation and transmission. In 2010 & 2011 we deployed 5 moorings (locations indicated at right in red) and executed detailed shipboard campaigns to:

- identify hotspots of generation and dissipation,
- quantify the structure and variability of wave energy, its flux and dissipation at the generation site.
- link the broader spatial structure, temporal content, and energetics of the internal wave field to the topography, forcing, and mesoscale influences (i.e., Kuroshio).



APPROACH

Much of the turbulent dissipation in Luzon Strait was anticipated to be deep, outside the range of tethered microstructure profilers, and evolving too rapidly for autonomous profilers. We have used a 2-fold approach to quantify this deep turbulence:

1. rapid profiles at abyssal depths are obtained using standard shipboard CTD, augmented with ADCPs, turbulence sensors, and a motion package. These allow us to systematically obtain 36-h yo-yo timeseries, from which internal wave energy generation, transport and dissipation can be directly measured.
2. Five moorings were successfully deployed and recovered in 2 of the most energetic regions of the strait. Moorings had rapidly-sampled sensors with motion packages that permit turbulent dissipation to be computed in addition to the standard measurements used to assess internal wave energetics.

WORK COMPLETED

We have developed a self-contained microstructure package that can be lowered on a standard shipboard CTD to measure full water column turbulence. χ pod-CTD is a deep version of our equatorial-moored χ pod (Moum and Nash, 2009), with two fast-response thermistors, a full motion package and 3000-m depth rating. It is installed on the ship's CTD rosette, which is vanned to set χ pod's orientation into the flow. With the addition of 2-300 kHz ADCPs, this system measures full-water column velocity, density, and temperature microstructure, permitting dissipation rates of temperature variance (χ) and TKE (ϵ) to be computed.

This system was used for turbulence profiling during the 2010 IWISE pilot (Aug/Sept 2010), and on 4 cruises during the main IWISE-2011 experiment. O(500) profiles have been used for analysis to investigate the generation of internal waves, NLIWs, bores and their associated dissipation within Luzon Strait. In addition, one full water-column mooring and four near-bottom moorings were deployed at the central ridge crest and western ridge crest; the hardware for these were funded through our related DURIP. All deployed instruments were recovered except for one ADCP, which unfortunately broke free and was lost.

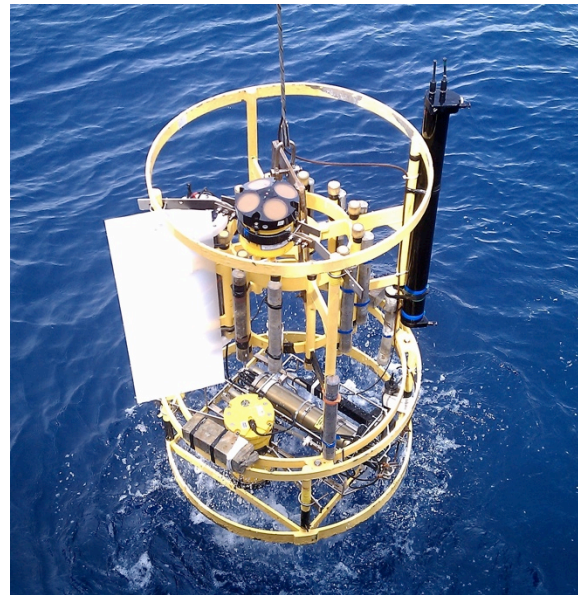


Figure 1: Revelle's CTD as modified during the IWISE pilot to measure full-depth velocity and dissipation rates. 2 ADCPS, a white vane for stabilization, and black χ pod are each visible.

RESULTS

Part 1: System-wide energy, flux and dissipation from shipboard CTD/LADCP.

As reported in Alford et al (2011), the results are spectacular. From an instrumentation standpoint, χ pod-CTD/LADCP returned uncontaminated temperature and its gradient on all upcasts during 2010. In 2011, the system was rebuilt to provide greater flexibility for sensor location in order to produce uncontaminated dissipation profiles on both up and down-casts. These have enabled the dissipation rates of temperature variance (χ) and TKE (ϵ) to be computed to 3000-m depths. A comparison of station-mean dissipation rates from χ pod and from Thorpe-scale estimates (figure 2) illustrates the strength of this methodology. At abyssal depths, dissipation estimates are consistent in their time-means, but differ in the details (since they are computed from different stages of turbulent-billow evolution). In the higher stratification surface waters, Thorpe estimates are biased low due to sensor resolution issues. In the 2011 field season, several hundred additional profiles were acquired, with 160 of them being at the same time/locations as L. St. Laurent's deep microstructure profiler (DMP), which permit direct statistical comparisons to be made.

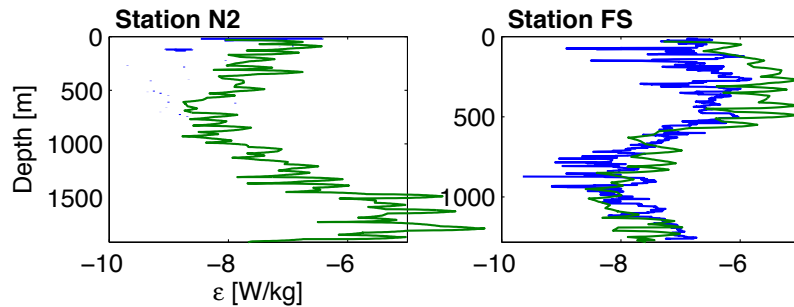


Figure 2: TKE dissipation rate from LADCP/ χ pods (green) and Thorpe analyses (blue) at two of the most energetic stations observed during the Luzon Strait pilot. These represent the first direct measurements of abyssal turbulence from shipboard CTD/LADCP.

Station N2a

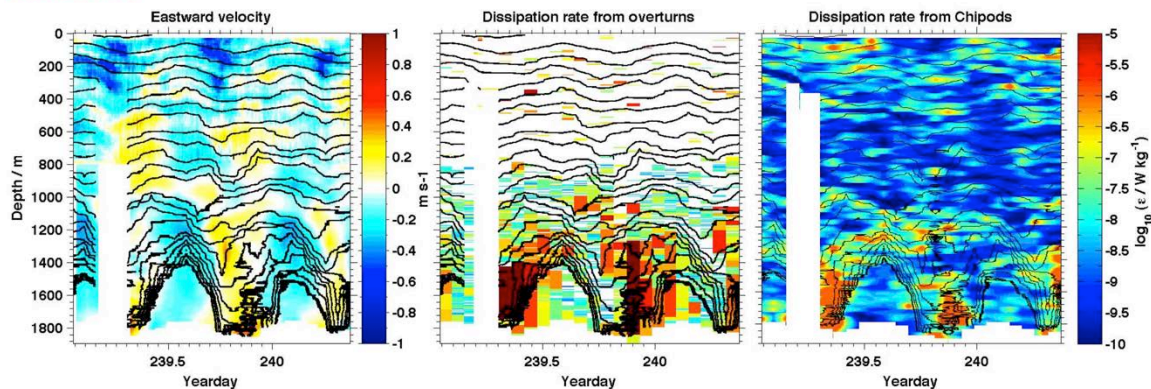


Figure 3 – Timeseries of velocity (left) and TKE dissipation from Thorpe overturns (middle) and from χ (right) for the first occupation of station N2. This was one of the more energetic stations, with vertical displacements and overturns exceeding 500 m, as illustrated by density contours (black).

Within the Strait, internal wave vertical displacements exceed 500 m and TKE dissipation rates are among the largest recorded in the abyssal ocean, exceeding 3×10^{-6} W/kg as the newly-generated internal tide interacts with the Western ridge at 1200-1800 m water depths (figure 3). In the upper water column, differences between dissipation rates computed from Thorpe-scales (Fig 3, center), and χ pods are due to Thorpe-estimate resolution; however, deep in the water column, these differences are real and provide important clues as to the mechanism and evolution of the turbulent overturns. These dynamics appear to have significantly more nonlinearity and dissipation than other sites of strong internal tide generation, such as the Hawaiian Ridge system (Nash et al 2006; Klymak et al, 2006).

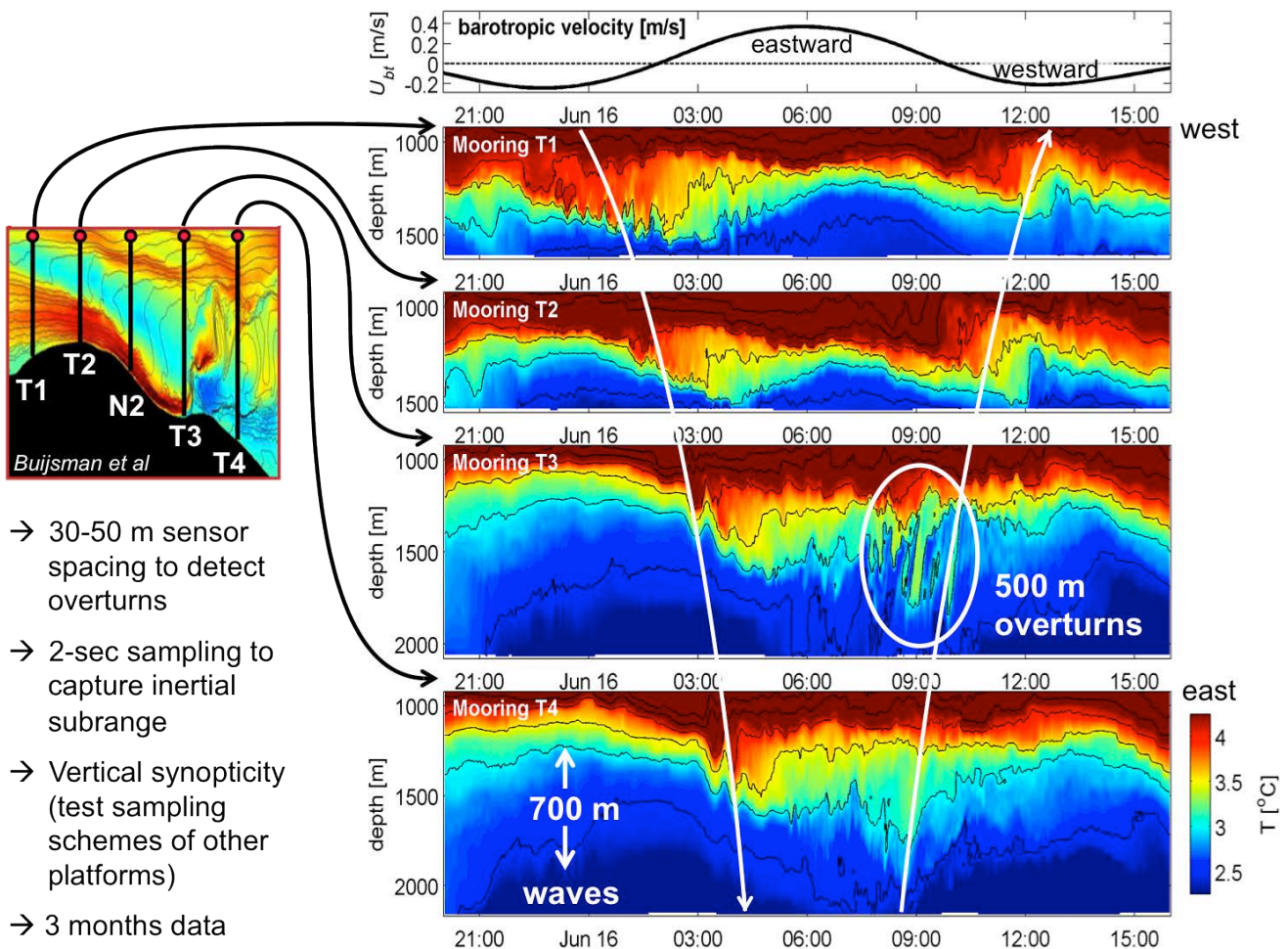


Figure 4: Main panels show temperature from the 4 T-chains deployed over the ridge near N2. These moorings were spaced 1 km apart and capture displacements and turbulence in x,z,t space. The inset (left) shows a snapshot of the spatial structure as captured by the numerical simulations of Maarten Buijsman. Our observations (right) rival numerical simulations in their temporal and vertical resolution, but represent the true reality and breadth of scales of the real ocean. These figures show the evolution and spatial structure of a 300-m tall wave which grows to 700 m in amplitude before it breaks, forming 500-m tall overturns. Short-wavelength features are coherent across the mooring array and can be tracked (white arrows).

Part 2: Moored T-chains and χ pods at Hang-Chun Ridge (West Ridge).

One focus of our 2011 observations was the structure of wave and dissipation events on Hang-Chun Ridge, near station N2. At that site, 5 moorings were deployed at 1-km spacing to capture the evolution of billowing as the waves break at the ridge crest. An example of a 20-h period from these moorings is shown in figure 4.

The above example represents one 20-h time window within the 3-month deployment. These records are analyzed in detail to quantify both internal wave and turbulent components. From these 0.5 Hz data, turbulent dissipation is inferred from Thorpe-scale analysis of unstable overturns. In addition, using direct turbulence data acquired from χ pods integrated into Alford's moored profilers (Moum & Nash), we are able to validate our Thorpe-based estimated of dissipation rates. From these combined data, we characterize the evolution of turbulence throughout the spring/neap cycle (figure 5), which is based on a combination of Thorpe-based estimates (at T1-T4), direct turbulence observations (at N2), and comparisons to model simulations (Buijsman et al, 2013).

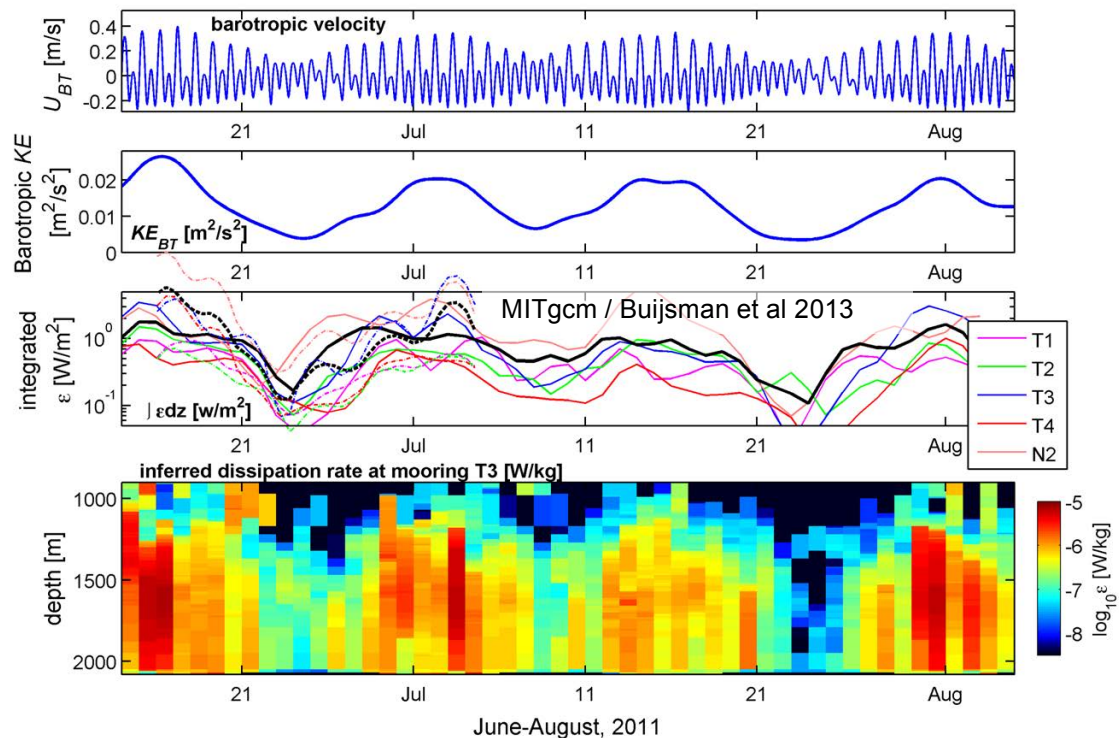
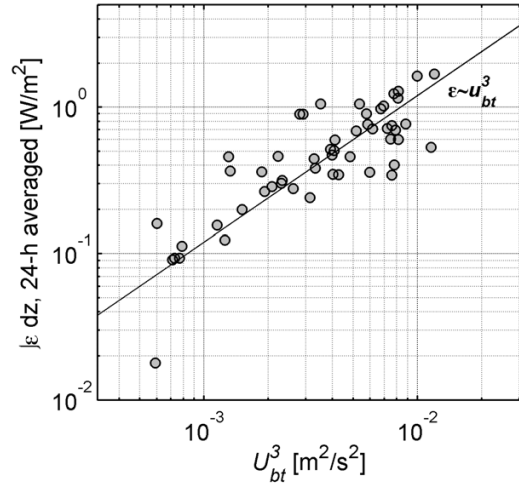


Figure 5: Evolution of dissipation throughout the spring/neap cycle. Top two panels show the barotropic tidal velocity and kinetic energy (KE) at the East Ridge, which represents the strength of the forcing. The lower panel shows the TKE dissipation (inferred from Thorpe scales) at the West Ridge mooring T3, which spans almost 3 orders of magnitude, even in 24-h averages. As a result, the depth-integrated dissipation exhibits a strong spring-neap cycle. This is summarized in the 3rd panel, which shows the observed depth integrated dissipation at the 5 West Ridge moorings (solid lines) along with that associated with MITgcm numerical simulations performed (Buijsman et al, 2014). The latter show similar trends, yet with magnitudes that differ slightly.

Figure 6: Scaling dissipation over Hang-Chun Ridge (the west ridge). Spatially-averaged, depth integrated dissipation scales strongly with the cube of the barotropic velocity, which provides strong support for the conceptual model of Klymak et al, 2010, who suggest that all trapped lee-waves will break quasi-locally, which leads to a scaling whereby dissipation scales with u^3 .



Ridge-integrated dissipation is found to scale with the cube of velocity (figure 6), supporting the simple parameterizations for turbulence suggested by Klymak et al (2010). Combining all of these data at the west ridge, we generate a composite picture of the mean displacements and TKE dissipation rate during periods where either the diurnal or semidiurnal tides dominate the forcing (figure 7). While displacements during both periods are dominated by semidiurnal variability, the dissipation is strongly diurnal, and these signals dominate the time averages. This highlights the fact that the details of how semidiurnal and diurnal signals beat together represent a strong control on the total dissipation.

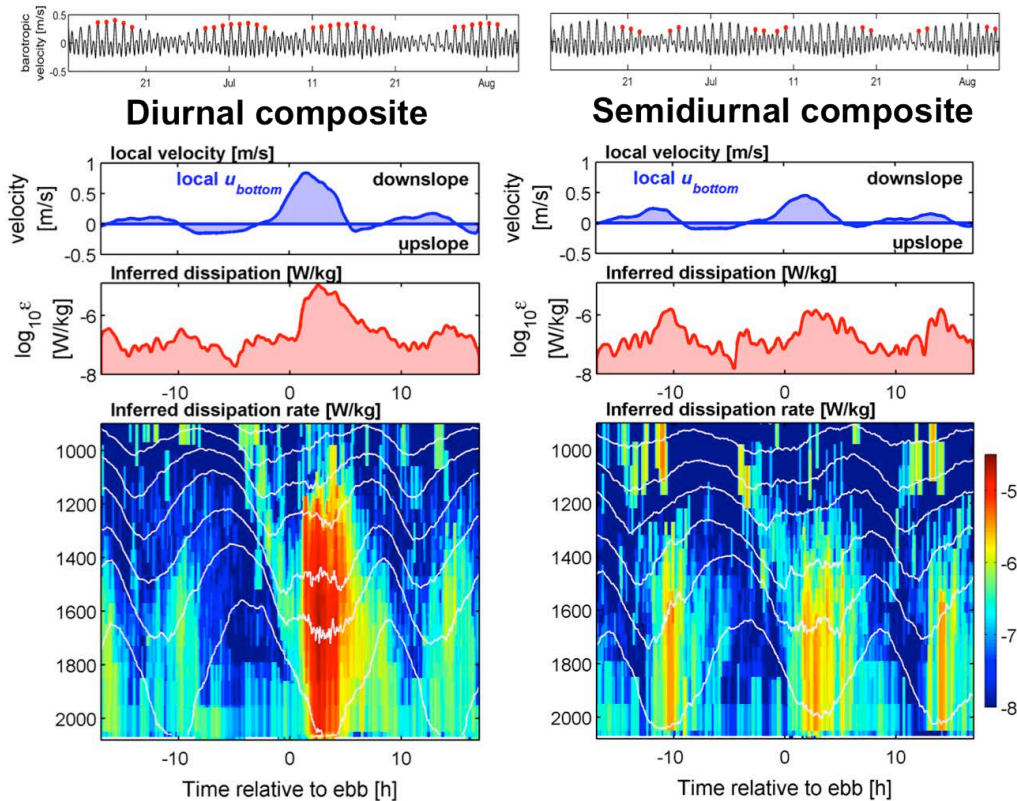


Figure 7: tidal composites of near-bottom velocity (middle-top), and mean dissipation rate (lower panels) for two different periods where the forcing is either dominated by the diurnal tide (left) or the semidiurnal tide (right). Red dots in the upper panels show the tidal cycles over which the composites were generated.

Part 3: Stablemoor (mooring A1) and χ pods at Lan-Yu Ridge (the East Ridge).

The tidal transports, internal tide generation and internal tide at Lan-Yu Ridge are some of the largest ever sampled by an extended-deployment, full water column mooring. Using our unique stablemoor float – which is a platform for both turbulence and acoustics measurements – we are able to directly quantify internal wave fluxes (figure 8), energy dissipation (figure 9-10) and irreversible transports (see Moum/Nash annual report). A dominant theme in all of these analyses is the importance of the spring/neap cycle in controlling the energetics (figure 8). An emerging result is how the various components of the tide (semidiurnal, diurnal), and the mesoscale add nonlinearly so that the ratio of energy dissipated to energy converted from the barotropic tide depends strongly on the strength of the forcing. Moreover, the details of how the diurnal and semidiurnal motions superimpose (i.e., the way they beat together) is found to control the rate of dissipation (figure 10).

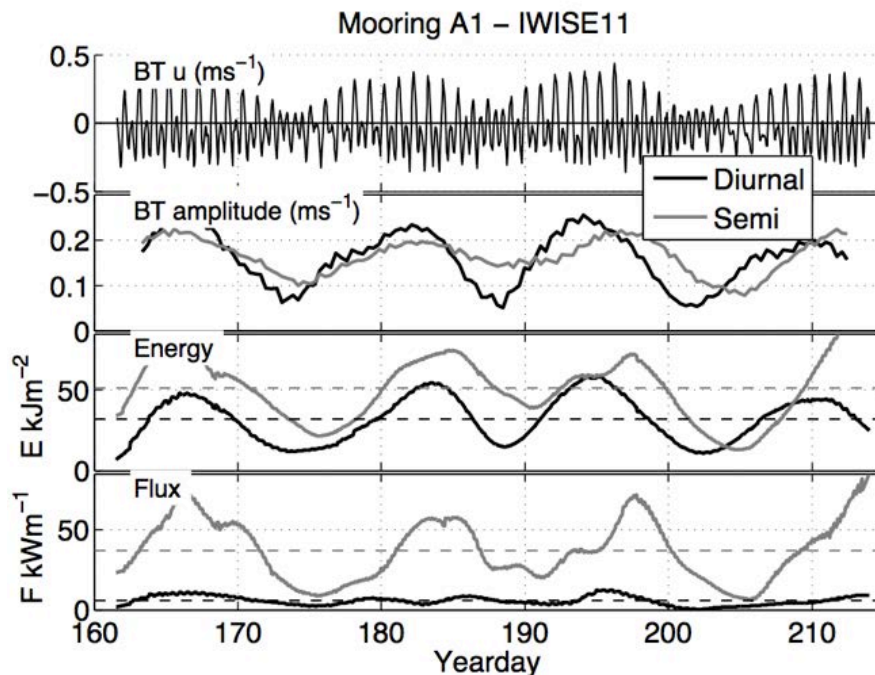


Figure 8: Baroclinic energy and energy flux along the north line of the Lan-Yu Ridge (from Pickering et al, 2012) exhibit strong spring/neap modulation, and illustrate how the internal tide energetics scales directly to the strength of the barotropic forcing. Here we've separated diurnal and semidiurnal contributions; the ratio of the flux to energy in each of these bands is used to assess the degree to which each of these forms standing vs. propagating modes.

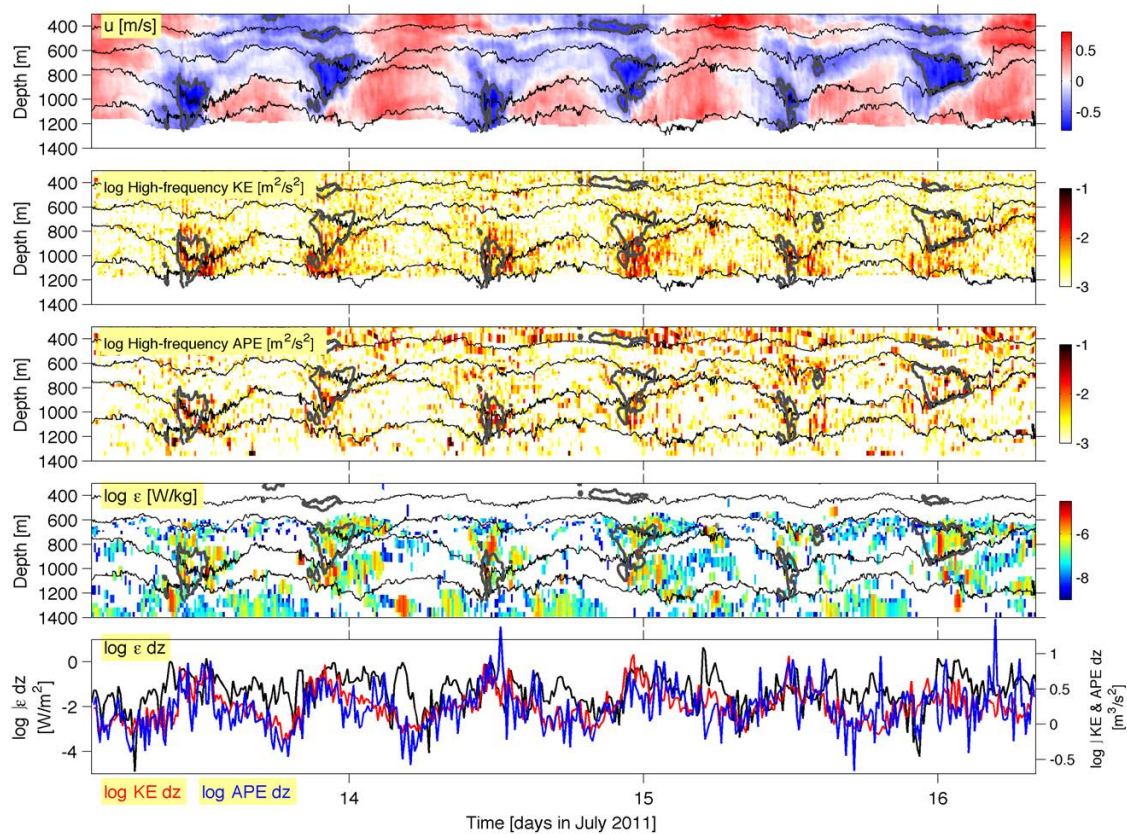


Figure 9: Velocity, high-frequency KE, APE and turbulent dissipation at mooring A1 on the Lan-Yu Ridge. High dissipation events appear to be linked to fluctuations in velocity and displacement, as characterized by the energy at periods shorter than 15 minutes. (from Lim et al, 2014).

Fifty fast-response thermistors and CTD sensors distributed throughout the water column at mooring A1 permit dissipation to be estimated from Thorpe scales (figure 9). In addition, χ pods were placed at a few discrete locations, permitting comparisons and validation of the inertial subrange estimates. High-turbulence events are strongly tied to westward flow across Lan-Yu ridge, creating downstream lee waves to form, break and produce high levels of KE and APE. While the observed vertical displacements are dominated by the semidiurnal tides, the turbulence appears driven by the cube of the total velocity, which is strongly influenced by *both semidiurnal and diurnal forcing*.

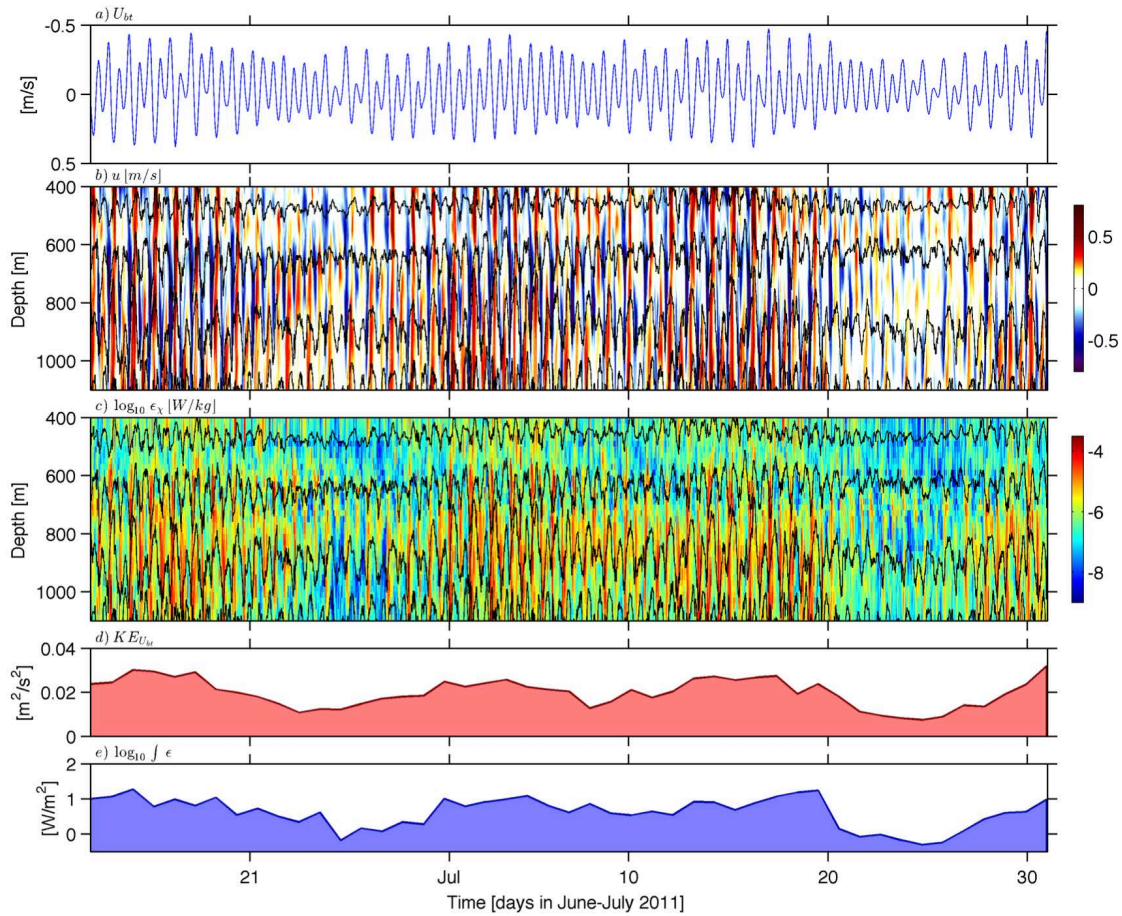


Figure 10: Forty-five day record of barotropic velocity (top), eastward velocity (2nd panel), inferred turbulent dissipation from Thorpe scales (3rd panel), barotropic KE (4th panel) and depth-integrated dissipation (bottom panel).

Over longer time scales (figure 10), the spring-neap cycling of turbulence is evident, driven by the beating between the various diurnal and semidiurnal constituents. Most striking is the contrast in dissipation rates between diurnally-dominated springs on July 16 and the very weak neap tides 7 days later, when the cross ridge was reduced by a factor of 2, producing a drop in dissipation by almost 2 orders of magnitude.

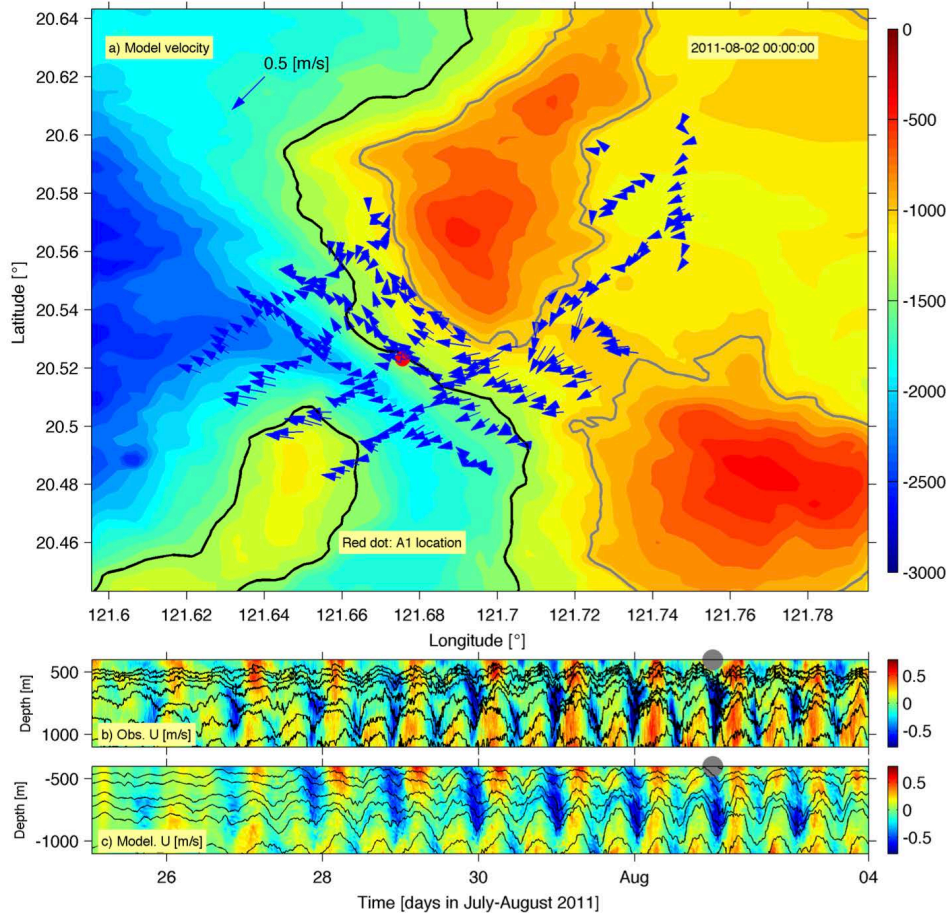


Figure 11: Numerically-simulated near-bottom velocities show complicated 3D flow patterns in the vicinity of mooring A1 (red dot), one of the primary internal tide generation sites in the Strait (Buijsman et al, 2014). Timeseries of velocity (bottom) indicate that the observations (2nd panel) and model (3rd panel) are strongly correlated, yet the model produces weaker flows and less-sharp transitions at the tidal reversals.

Summary:

This observational program has:

1. provided an exceptionally detailed perspective on the generation, structure and dissipation of internal tides in one of the most energetic regions of the world;
2. captured perhaps the largest breaking waves in the ocean, characterizing the spatial and temporal variability of their dissipation; and
3. assessed the accuracy of numerical predictions in capturing small-scale dynamics. One particular focus is quantifying the effectiveness of both complicated and simple turbulence parameterizations.

RELATED PROJECTS

Profiling and moored operations are being coordinated with M Alford and A Pickering (UW); analysis of turbulence data are being conducted in conjunction with J MacKinnon (UCSD), H Simmons (UAF) and L. St. Laurent (WHOI). Data/model integration and comparisons are being made with Simmons, Klymak, and Buijsman.

SYNERGIES

This award funded the development of the χ pod-CTD, which was used throughout IWISE-2010 and IWISE-2011, and in the Bay of Bengal (ASIRI) on both US and Indian research vessels. The success of these measurements led us to develop a second-generation system, which Nash, Moum and MacKinnon have obtained funding for through NSF. Several new systems are being fabricated and will be installed/ deployed on ship-based CTD rosettes as part of the global repeat hydrography program over the next several years. The ultimate goal is to obtain thousands of turbulence profiles during routine hydrographic surveys (distributed globally) using the instruments originally developed through this award.

REFERENCES

- Klymak, J.M., J.N. Moum, J.D. Nash, E. Kunze, J.B. Girton, G.S. Carter, C.M. Lee, T.B. Sanford, and M.C. Gregg, 2006: An estimate of tidal energy lost to turbulence at the Hawaiian Ridge. *J. Phys. Oceanogr.*, 36, 1148-1164.
- Klymak, J. M., S. Legg, and R. Pinkel, 2010: A simple parameterization of turbulent tidal mixing near supercritical topography. *J. Phys. Oceanogr.*, 40(9):2059-2074, doi:10.1175/2010JPO4396.1.
- Moum, J.N. and J.D. Nash, 2009: Mixing measurements on an equatorial ocean mooring, *J. Atmos. and Oceanic Tech.*, 26, 317-336.
- Nash, J.D., E. Kunze, C.M. Lee and T.B. Sanford, 2006: Structure of the baroclinic tide generated at Kaena Ridge, Hawaii, *J. Phys. Oceanogr.*, 36(6), 1123-1135.
- Zhang, Y. and J.N. Moum, 2010: Inertial-convective subrange estimates of thermal variance dissipation rate from moored temperature measurements. *J. Atmos. Oceanic Technol.*, 27, 1950–1959.

PUBLICATIONS

- Alford and 40 coauthors, 2014: The formation and fate of internal waves in the South China Sea, *Nature* [under review]
- Nash and coauthors, 2014: The Anatomy and Implications of Turbulence in Huge Undersea Breaking Waves, *Nature* [in prep]

- Pickering, A., M.H. Alford, L. Rainville, J.D. Nash, B. Lim, M. Buijsman and D.S.Ko, 2014: Structure and Variability of Internal Tides in Luzon Strait, *J. Phys Oceanogr.* [in prep]
- Lim, B., J.D. Nash, J.N. Moum, 2014: Turbulent dissipation at a site of intense internal tide generation, *J. Phys. Oceanogr.* [in prep]
- Buijsman, M, J.M Klymak, S. Legg, M.H. Alford, D.A. Farmer, J.A. MacKinnon, J.D. Nash, J-H Park, A. Pickering, H. Simmons, 2014. Three Dimensional Double Ridge Internal Tide Resonance in Luzon Strait. *J. Phys. Oceanogr*, 44, 850-869. [published]
- Alford, M.H., J.A. MacKinnon, J.D. Nash, H. Simmons, A. Pickering, J.M. Klymak, R. Pinkel, O. Sun, L. Rainville, R. Musgrave, T. Beitzel, K-H Fu and C-W Lu, 2011: Energy flux and dissipation in Luzon Strait: two tales of two ridges. *J. Phys. Oceanogr.* doi: 10.1175/JPO-D-11-073.1 [published]
- Buijsman, M.C., S. Legg and J.M. Klymak, 2012: Double-Ridge Internal Tide Interference and Its Effect on Dissipation in Luzon Strait. *J. Phys. Oceanogr.*, 42, 1337–1356. doi: <http://dx.doi.org/10.1175/JPO-D-11-0210.1> [published]
- Kelly, S. M., N. L. Jones, J. D. Nash, and A. F. Waterhouse, 2013: The geography of semidiurnal mode-1 internal-tide energy loss, *Geophys. Res. Lett.*, 40, doi:10.1002/grl.50872. [published]
- Nash, J.D., S.M. Kelly, E.L. Shroyer, J. N. Moum, and T. F. Duda, 2012: The unpredictable nature of internal tides and nonlinear waves on continental shelves. *J. Phys. Oceanogr.*, 42, doi: 10.1175/JPO-D-12-028.1 [published]
- Nash, J.D., E.L. Shroyer, S.M. Kelly, M.E. Inall, T.F. Duda, M.D. Levine, N.L. Jones, and R.C. Musgrave, 2012: Are any coastal internal tides predictable? *Oceanography*, 25(2) 80-95. [published]
- Klymak, J.M., S. Legg, M.H. Alford, M. Buijsman, R. Pinkel, and J.D. Nash, 2012: The direct breaking of internal waves at steep topography. *Oceanography*, 25(2) 150-159. [published]